ISSN 0915-633X

NATIONAL INSTITUTE FOR FUSION SCIENCE

Soliton on Thin Vortex Filament

K. Konno, M. Mituhashi and Y. H. Ichikawa

(Received – Nov. 5, 1990)

NIFS-63 Dec. 1990

RESEARCH REPORT
NIFS Series

NAGOYA, JAPAN

Soliton on Thin Vortex Filament

Kimiaki KONNO, Masahiko MITUHASHI* and Yoshi H. ICHIKAWA†

Department of Physics,
College of Science and Technology,
Nihon University,
Chiyoda-ku
Tokyo 101.
*Industrial Research Institute of Kanagawa,
Kanazawa-ku,
Yokohama 236.
†National Institute for Fusion Science,
Chikusa-ku,
Nagoya 464-01.

Abstract:

Showing that one of the equations found by Wadati, Konno and Ichikawa is equivalent to the equation of motion of a thin vortex filament, we investigate solitons on the vortex filament. N vortex soliton solution is given in terms of the inverse scattering method. We examine two soliton collision processes on the filament. Our analysis provides the theoretical foundation of two soliton collision processes observed numerically by Aref and Flinchem.

Keywords: soliton, thin vortex filament, vortex soliton
inverse scattering transformation,

§ 1 Introduction

The inverse scattering method reveals itself as a powerful and useful tool to solve nonlinear integrable equations.[1] A generalization of the inverse scattering method was achieved by Wadati, Konno and Ichikawa.[2),3] So we can solve many interesting nonlinear equations and explore exotic solitons such as the spiky soliton, the cusp soliton and the loop soliton.[4]

In Ref. 3 we found two types of new integrable equations (WKI equations in short). The first of the equations for the real variable is shown to describe loop soliton.[5),6] We illustrated a small loop soliton traveling along a large loop soliton. We will discuss here soliton solutions of the second of the equations. Basing on the inverse scattering method, Shimizu and Wadati[7] discussed the cusp soliton solution of the second type of the WKI equations. In this paper, we will modify the equation to allow a complex multivalued solution by introducing a sign function in the same way as we modified the first type of the WKI equations to obtain the loop soliton.

The modified equation will be proofed to be equivalent to the equation of motion of a thin vortex filament[8] so that the solution represents the vortex soliton on the filament. The vortex soliton have been conventionally described by the nonlinear Schrödinger equation based on the curvature and torsion of the vortex.[9] On the other hand, Levi, Sym and Wojciechowski have discussed the solution by their geometric method.[10] However these approaches were rather complicated to get explicit form of solution. In this connection Aref and Flinchem have carried out numerical solution of the equation of the vortex filament motion.[11] Having proofed that the equation of motion of the vortex filament is nothing but the second type of the WKI equations, here we can carry out rigorous analysis of collision process of vortex solution. We will find three kinds of vortex soliton solutions such as lump soliton, cusp soliton and multivalued loop soliton depending on the eigenvalue of the inverse scattering method. With such a variety of solitons, we can analyze details of complex behavior of collision processes.

In § 2 we will discuss modification of the second type of the WKI equations and show equivalence of it to the equation of motion of a thin vortex filament. We will discuss the inverse scattering method in § 3 and will derive an N vortex soliton solution in § 4. Collision processes of two solitons in the three dimensional space are studied in § 5. The final section is devoted to discussions.

§ 2 Equation of Motion of Thin Vortex Filament

Let us first derive the equation of motion of a thin vortex filament from the following modified WKI equation:

$$i\,\frac{\partial^2 q}{\partial t \partial x} + sgn\left(\frac{dx}{ds}\right)\frac{\partial^2}{\partial x^2}\left(\frac{\frac{\partial q}{\partial x}}{\Phi}\right) = 0\ . \tag{2.1}$$

where

$$\Phi = \sqrt{1 + \left|\frac{\partial q}{\partial x}\right|^2}\ . \tag{2.2}$$

Here we introduced the sign function $sgn(dx/ds)$ where ds is the element of the arc length along of solution curve:

$$ds = \sqrt{(dx)^2 + |dq|^2}\ . \tag{2.3}$$

It is crucial to attach the sign function to discuss multivalued solution. For the loop type of deformation, dx takes negative value at the upper part of a loop, while ds is positive definite. Furthermore in order to follow such a deformation we find that it is effective to transform independent variables from (x,t) to (s,t) with the definition of s:

$$s = x + \int_x^\infty \left(1 - sgn\left(\frac{dx}{ds}\right)\Phi\right) dx\ . \tag{2.4}$$

Taking the variation ds from Eq.(2.4), we get Eq.(2.3) and thus confirm the consistency of the definition of the independent variable s.

Introduce the the tangent vector $\mathbf{t}$ defined by $\partial \mathbf{r}/\partial s$ as

$$\mathbf{t} = \frac{\partial \mathbf{r}}{\partial s} = \left(\frac{\partial x}{\partial s}, -\mathrm{Im}\,\frac{\partial q}{\partial s}, \mathrm{Re}\,\frac{\partial q}{\partial s}\right)\ , \tag{2.5}$$

where $\mathbf{r}$ is a position vector in the three dimensional space given as

$$\mathbf{r} = (x, -\mathrm{Im}\,q, \mathrm{Re}\,q)\ . \tag{2.6}$$

The equation of motion of a thin vortex filament[8] is given by

$$\frac{\partial \mathbf{t}}{\partial t} = \mathbf{t} \times \frac{\partial^2 \mathbf{t}}{\partial s^2}\ . \tag{2.7}$$

Taking a ratio of two components of the tangent vector such as $t_y/t_x = \partial q/\partial x$ and calculating time evolution of the ratio in accordance with Eq.(2.7), we obtain a transformed equation of Eq.(2.1) expressed by the independent variables (s,t) and thus we can verify that Eq.(2.1) is equivalent to Eq.(2.7).[12] We also notice that the size of the tangent vector is unity as

$$\mathbf{t}^2 = \frac{(dx)^2 + |dq|^2}{(ds)^2} = 1 . \tag{2.8}$$

Integrating Eq.(2.7) with respect to s, we get

$$\frac{\partial \mathbf{r}}{\partial t} = \frac{\partial \mathbf{r}}{\partial s} \times \frac{\partial^2 \mathbf{r}}{\partial s^2} , \tag{2.9}$$

for which Aref and Flinchem carried out their numerical computation. Now we are able to construct solution of Eq.(2.9) as soliton solution of Eq.(2.1). In the next section we will derive N soliton solution of Eq.(2.1) by using the inverse scattering method.

§ 3 Inverse Scattering Problem

With the inverse scattering method, we solve Eq.(2.1) under the boundary conditions

$$\left.\begin{aligned} q &\to 0 , \\ \frac{\partial q}{\partial x} &\to 0 , \end{aligned}\right\} \quad as \quad |x| \to \infty . \tag{3.1}$$

The eigenvalue problem is given by

$$\begin{aligned} \frac{\partial v_1}{\partial x} + i\lambda v_1 &= \lambda \frac{\partial q}{\partial x} v_2 , \\ \frac{\partial v_2}{\partial x} - i\lambda v_2 &= -\lambda \frac{\partial q^*}{\partial x} v_1 , \end{aligned} \tag{3.2}$$

where the time dependence of the eigenfunctions has the forms

$$\begin{aligned} \frac{\partial v_1}{\partial t} &= A v_1 + B v_2 , \\ \frac{\partial v_2}{\partial t} &= C v_1 - A v_2 , \end{aligned} \tag{3.3}$$

in which

$$A = sgn\left(\frac{dx}{ds}\right)\left(\frac{2i}{\Phi}\lambda^2\right) ,$$

$$B = sgn\left(\frac{dx}{ds}\right)\left(2\frac{\frac{\partial q}{\partial x}}{\Phi}\lambda^2 + i\frac{\partial}{\partial x}\left(\frac{\frac{\partial q}{\partial x}}{\Phi}\right)\lambda\right) , \tag{3.4}$$

$$C = sgn\left(\frac{dx}{ds}\right)\left(-2\frac{\frac{\partial q^*}{\partial x}}{\Phi}\lambda^2 + i\frac{\partial}{\partial x}\left(\frac{\frac{\partial q^*}{\partial x}}{\Phi}\right)\lambda\right) .$$

The Gel'fand-Levitan equation can be obtained on the same way as Ref. 7. We sketch the process. Define the Jost functions:

$$\left.\begin{array}{l} \phi \rightarrow \begin{pmatrix} 1 \\ 0 \end{pmatrix} , \\ \bar{\phi} \rightarrow \begin{pmatrix} 0 \\ -1 \end{pmatrix} , \end{array}\right\} \quad \text{as} \quad x \rightarrow -\infty, \tag{3.5}$$

and

$$\left.\begin{array}{l} \psi \rightarrow \begin{pmatrix} 0 \\ 1 \end{pmatrix} , \\ \bar{\psi} \rightarrow \begin{pmatrix} 1 \\ 0 \end{pmatrix} , \end{array}\right\} \quad \text{as} \quad x \rightarrow \infty \tag{3.6}$$

and the scattering coefficients:

$$\begin{aligned} \phi &= a\,\bar{\psi} + b\psi , \\ \bar{\phi} &= -\,\bar{a}\,\psi + \bar{b}\,\bar{\psi} , \end{aligned} \tag{3.7}$$

where

$$a\,\bar{a} + b\,\bar{b} = 1 . \tag{3.8}$$

In order to examine the analytic properties of the Jost functions for large $|\lambda|$ we introduce[13)]

$$\phi_1 = exp\{-i\lambda x + \int_{-\infty}^{x} \sigma(\lambda, x')\, dx'\} . \tag{3.9}$$

Substitution of Eq.(3.9) into Eq.(3.2) together with Eq.(3.3) then yields

$$\frac{\partial \sigma}{\partial t} = \frac{\partial}{\partial x}\left(A + \frac{\sigma}{\lambda\frac{\partial q}{\partial x}}B\right) . \tag{3.10}$$

If we expand σ as an inverse power series in λ of the form

$$\sigma = \sum_{n=-1}^{\infty} \frac{\sigma_n}{(i\lambda)^n} , \tag{3.11}$$

we obtain an infinite number of conserved quantities by substituting Eq.(3.11) into Eq.(3.10). The following first two conserved quantities play a crucial role to express asymptotic behavior of the Jost functions:

$$\sigma_{-1} = 1 - sgn\left(\frac{dx}{ds}\right)\Phi ,$$

$$\sigma_0 = -\frac{\dfrac{\partial^2 q}{\partial x^2}}{2\dfrac{\partial q}{\partial x}}\left\{sgn\left(\frac{dx}{ds}\right)\frac{1}{\Phi} - 1\right\} - \frac{1}{2}\frac{\partial}{\partial x}\log\Phi , \tag{3.12}$$

which vanish for $|x| \to \infty$. Then the asymptotic form of ϕ and a for large $|\lambda|$ are written as

$$\phi = \begin{pmatrix} 1 \\ i\sigma_{-1}/\frac{\partial q}{\partial x} \end{pmatrix} \exp\{-i\lambda x + i\lambda\varepsilon_- + \mu_-\} + O\left(\frac{1}{\lambda}\right) , \tag{3.13}$$

$$a = \exp(i\lambda\varepsilon + \mu) + O\left(\frac{1}{\lambda}\right) , \tag{3.14}$$

where

$$\begin{aligned} \varepsilon = \varepsilon_- + \varepsilon_+ &= \int_{-\infty}^{\infty} \sigma_{-1}\, dx , \quad & \varepsilon_- &= \int_{-\infty}^{x} \sigma_{-1}\, dx , \quad & \varepsilon_+ &= \int_{x}^{\infty} \sigma_{-1}\, dx , \\ \mu = \mu_- + \mu_+ &= \int_{-\infty}^{\infty} \sigma_0\, dx , \quad & \mu_- &= \int_{-\infty}^{x} \sigma_0\, dx , \quad & \mu_+ &= \int_{x}^{\infty} \sigma_0\, dx . \end{aligned} \tag{3.15}$$

On the same way we can obtain the asymptotic behavior of $\bar{\phi}$, ψ and $\bar{\psi}$.

Use the fact that $\phi\exp\{i\lambda(x - \varepsilon_-)\}$, $\bar{\phi}\exp\{-i\lambda(x - \varepsilon_-)\}$, $\psi\exp\{-i\lambda(x + \varepsilon_+)\}$, $\bar{\psi}\exp\{i\lambda(x + \varepsilon_+)\}$ and $a\exp(-i\lambda\varepsilon)$ are entire functions of λ and introduce the kernels K_1 and K_2:

$$\begin{aligned} \begin{pmatrix} \bar{\psi}_1 \\ \bar{\psi}_2 \end{pmatrix} &= \begin{pmatrix} 1 \\ 0 \end{pmatrix} \exp\{i\lambda(x + \varepsilon_+(x) - \mu_+^*(x))\} \\ &+ \int_x^{\infty} \begin{pmatrix} \lambda K_1(x,z)\exp\{-\mu_+(x)\} \\ K_2(x,z)\exp\{-\mu_+^*(x)\} \end{pmatrix} \exp\{i\lambda(z + \varepsilon_+(x))\}\, dz , \end{aligned} \tag{3.16}$$

where we shall assume

$$\lim_{z\to\infty} K_1(x,z) = 0 \ , \quad \lim_{z\to\infty} K_2(x,z) = 0 \ . \tag{3.17}$$

We have

$$K_1(x,x) = \frac{\sigma_{-1}}{\frac{\partial q^*}{\partial x}} \exp(\mu_+ - \mu_+^*) \ , \tag{3.18}$$

and the Gel'fand-Levitan equations for $x \geq y$:

$$\begin{aligned} &K_1(x,y) - F^*(x+y) - \int_x^\infty F^*(y+z)\, K_2^*(x,z)\, dz = 0 \ , \\ &K_2^*(x,y) - \int_x^\infty F''(y+z)\, K_1(x,z)\, dz = 0 \ , \end{aligned} \tag{3.19}$$

where

$$\begin{aligned} F(z) &= \frac{1}{2\pi} \int_c \frac{b(\lambda)}{\lambda\, a(\lambda)} \exp\{i\lambda(z + 2\varepsilon_+(x))\}\, d\lambda \ , \\ F''(z) &= \frac{\partial^2 F}{\partial z^2} = -\frac{1}{2\pi} \int_c \frac{\lambda\, b(\lambda)}{a(\lambda)} \exp\{i\lambda(z + 2\varepsilon_+(x))\}\, d\lambda \ . \end{aligned} \tag{3.20}$$

Here the contour c is defined to be the contour in the complex λ plane, starting from $-\infty + i0^+$, passing over all zeros of a and ending at $+\infty + i0^+$. Time dependence of the scattering data is given by

$$\begin{aligned} a(\lambda,t) &= a(\lambda,0) \ , \\ b(\lambda,t) &= b(\lambda,0) \exp(4i\lambda^2 t) \ . \end{aligned} \tag{3.21}$$

When all the zeros of $a(\lambda)$ in the upper half plane are simple, $F(z)$ can be expressed as

$$F(z) = \sum_{k=1}^{N} \frac{C_k(t)}{\lambda_k} \exp\{i\lambda_k(z + 2\varepsilon_+(x))\} + \frac{1}{2\pi} \int_{-\infty}^{\infty} \frac{\rho(\lambda,t)}{\lambda} \exp\{i\lambda(z + 2\varepsilon_+(x))\}\, d\lambda \ , \tag{3.22}$$

where

$$\begin{aligned} C_k(t) &= C_k(0) \exp(4i\lambda_k^2 t) \ , \\ \rho(\lambda,t) &= \rho(\lambda,0) \exp(4i\lambda^2 t) \ . \end{aligned} \tag{3.23}$$

Giving the scattering data $\{\rho(\lambda,0), \lambda;\ C_k(0), \lambda_k, k = 1,2,\ldots,N\}$, we can determine $F(z)$ and solve $K_1(x,x)$ with the Gel'fand-Levitan equations. We then obtain the solution by using the relation (3.18).

§ 4 N Soliton Solution

The N soliton solution is obtained under the conditions:

$$\begin{aligned} &(1) \quad \rho(\lambda, t) = 0 \ , \\ &(2) \quad \lambda_k \ , \qquad k = 1, 2, ..., N \ . \end{aligned} \tag{4.1}$$

Then $F(z,t)$ in Eq.(3.22) reduces to

$$F(z) = \sum_{k=1}^{N} \frac{C_k(t)}{\lambda_k} \exp\{i\lambda_k(z + 2\varepsilon_+(x))\} \ . \tag{4.2}$$

In order to solve the Gel'fand-Levitan equations, we introduce the representations

$$\begin{aligned} K_1 &= \sum_{k=1}^{N} A_k(x) \exp\{-i\lambda_k^*(x + y + 2\varepsilon_+(x))\} \ , \\ K_2 &= \sum_{k=1}^{N} B_k(x) \exp\{-i\lambda_k^*(x + y + 2\varepsilon_+(x))\} \ . \end{aligned} \tag{4.3}$$

Substituting Eqs.(4.2) and (4.3) into Eq.(3.19), we obtain

$$\begin{aligned} A_k - i\,\frac{C_k^*}{\lambda_k^*} \sum_{l=1}^{N} \frac{B_l^* \exp\{2i\lambda_l(x + \varepsilon_+(x))\}}{\lambda_l - \lambda_k^*} &= \frac{C_k^*}{\lambda_k^*} \ , \\ B_k^* + i\ C_k\lambda_k \sum_{l=1}^{N} \frac{A_l \exp\{-2i\lambda_l^*(x + \varepsilon_+(x))\}}{\lambda_l - \lambda_k^*} &= 0 \ . \end{aligned} \tag{4.4}$$

Then A_k is given by

$$A_k = \frac{||D_k||}{||D||} \ . \tag{4.5}$$

Here the determinant $||D||$ of the 2N×2N matrix is defined as

$$||D|| = \begin{vmatrix} I & G \\ H & I \end{vmatrix} \ , \tag{4.6}$$

with the N×N matrices I, G and H of the elements

$$\begin{aligned} I_{kl} &= \delta_{kl} \\ G_{kl} &= -i\frac{C_k^* \exp\{2i\lambda_l(x + \varepsilon_+(x))\}}{\lambda_k^*(\lambda_l - \lambda_k^*)} \ , \\ H_{kl} &= i\frac{C_k\lambda_k \exp\{-2i\lambda_l^*(x + \varepsilon_+(x))\}}{\lambda_l - \lambda_k^*} \ , \end{aligned} \tag{4.7}$$

while the determinant $||D_k||$ is given by replacing the k-th column of $||D||$ by the element $(C_1^*/\lambda_1^*,\ldots,C_n^*/\lambda_n^*,0,\ldots,0)$. Thus

$$K_1(x,x) = \sum_{k=1}^{N} \frac{||D_k|| \exp\{-2i\lambda_k^*(x+\varepsilon_+(x))\}}{||D||} . \tag{4.8}$$

One should observe the dependence of $K_1(x,x)$ on $s = x + \varepsilon_+$ defined in Eq.(2.4). Thus both $q(s)$ and $\varepsilon_+(s)$ become single-valued functions even if $q(x)$ and $\varepsilon_+(x)$ are multivalued functions. We have

$$\begin{aligned} q &= \int_s^\infty \frac{2K_1}{1+|K_1|^2} \exp(\mu_+^* - \mu_+)\, ds \ , \\ \varepsilon_+ &= -\int_s^\infty \frac{2|K_1|^2}{1+|K_1|^2}\, ds \ , \\ \mu_+^* - \mu_+ &= -\int_s^\infty \frac{|K_1|^2}{1-|K_1|^2} \left(\frac{d}{ds} \log \frac{K_1}{K_1^*}\right) ds \ . \end{aligned} \tag{4.9}$$

$\mu_+^* - \mu_+$ can be integrated in such a form as

$$\mu_+^* - \mu_+ = \log \frac{||D||}{||D||^*} . \tag{4.10}$$

§ 5 Collision of Solitons in Three Dimensional Space

(a) One Soliton Solution

For one soliton solution with an eigenvalue $\lambda = \xi + i\eta$, q and ε_+ are give by

$$q = -i\frac{C^*}{\lambda^{*2}} \frac{\exp(-2i\lambda^* s)}{1 - \dfrac{|C|^2 \exp\{2i(\lambda-\lambda^*)s\}}{(\lambda-\lambda^*)^2}} \ ,$$

$$\varepsilon_+ = \frac{-i\dfrac{|C|^2 \exp\{2i(\lambda-\lambda^*)s\}}{|\lambda|^2(\lambda-\lambda^*)}}{1 - \dfrac{|C|^2 \exp\{2i(\lambda-\lambda^*)s\}}{(\lambda-\lambda^*)^2}} \ , \tag{5.1}$$

where

$$C = C(0)\exp(4i\lambda^2 t) \ . \tag{5.2}$$

The maximum amplitude of the soliton is given by $\eta/(\xi^2+\eta^2) = -\varepsilon/2$. The velocity v_s of the soliton in s coordinate is given by constant a -4ξ. However the velocity in x coordinate is not constant. It takes different values at different positions of the soliton and tends to be equal to v_s as $|x| \to \infty$ where ε_+ becomes constant. The solution changes its form with the period $\tau = \pi/\{2(\xi^2+\eta^2)\}$.

Corresponding to $|\xi| > \eta$, $|\xi| = \eta$ and $|\xi| < \eta$, we find three kinds of solutions such as lump, cusp and loop solitons, respectively. We note that the multiplicity of the solution originates from the fact that q depends on the S-shaped ε_+ function.[14] Depending upon the sign of the imaginary part of the eigenvalue the soliton travels upwards or downwards along the x axis. Since the phase factor at the maximum amplitude of a soliton is proportional to $\exp\{-4i(\xi^2+\eta^2)t\}$, then the direction of rotation to the x axis is clockwise with $\mathbf{r}$. We illustrate one loop soliton traveling to the negative direction together with ε_+ in Figure 1. Through this section we show stereographically the motion of the solitons with the coordinate $\mathbf{r}$ of Eq.(2.6).

Figure 1

(b) Two Soliton Solution

Two soliton solution is given by

$$\begin{aligned} q &= -i\frac{S}{R}, \\ \varepsilon_+ &= \frac{T}{R}, \end{aligned} \tag{5.3}$$

where

$$\begin{aligned} R = 1 &- \frac{|C_1|^2 \exp\{2i(\lambda_1-\lambda_1^*)s\}}{(\lambda_1-\lambda_1^*)^2} - \frac{|C_2|^2 \exp\{2i(\lambda_2-\lambda_2^*)s\}}{(\lambda_2-\lambda_2^*)^2} \\ &- \frac{C_1C_2^* \exp\{2i(\lambda_1-\lambda_2^*)s\}}{(\lambda_1-\lambda_2^*)^2} - \frac{C_1^*C_2 \exp\{2i(\lambda_2-\lambda_1^*)s\}}{(\lambda_2-\lambda_1^*)^2} \\ &+ \frac{|C_1|^2|C_2|^2|\lambda_1-\lambda_2|^4 \exp\{2i(\lambda_1-\lambda_1^*+\lambda_2-\lambda_2^*)s\}}{\{(\lambda_1-\lambda_1^*)(\lambda_1-\lambda_2^*)(\lambda_2-\lambda_1^*)(\lambda_2-\lambda_2^*)\}^2}, \end{aligned} \tag{5.4}$$

$$
\begin{aligned}
S = & \frac{C_1^* \exp(-2i\lambda_1^* s)}{\lambda_1^{*2}} + \frac{C_2^* \exp(-2i\lambda_2^* s)}{\lambda_2^{*2}} \\
& - \frac{|C_1|^2 C_2^* \lambda_1^2 (\lambda_1^* - \lambda_2^*)^2 \exp\{2i(\lambda_1 - \lambda_1^* - \lambda_2^*)s\}}{\{\lambda_1^* \lambda_2^* (\lambda_1 - \lambda_1^*)(\lambda_1 - \lambda_2^*)\}^2} \\
& - \frac{C_1^* |C_2|^2 \lambda_2^2 (\lambda_1^* - \lambda_2^*)^2 \exp\{2i(\lambda_2 - \lambda_1^* - \lambda_2^*)s\}}{\{\lambda_1^* \lambda_2^* (\lambda_2 - \lambda_1^*)(\lambda_2 - \lambda_2^*)\}^2} ,
\end{aligned}
\tag{5.5}
$$

and

$$
\begin{aligned}
T = & -i \frac{|C_1|^2 \exp\{2i(\lambda_1 - \lambda_1^*)s\}}{|\lambda_1|^2 (\lambda_1 - \lambda_1^*)} - i \frac{|C_2|^2 \exp\{2i(\lambda_2 - \lambda_2^*)s\}}{|\lambda_2|^2 (\lambda_2 - \lambda_2^*)} \\
& - i \frac{C_1 C_2^* \exp\{2i(\lambda_1 - \lambda_2^*)s\}}{\lambda_1 \lambda_2^* (\lambda_1 - \lambda_2^*)} - i \frac{C_1^* C_2 \exp\{2i(\lambda_2 - \lambda_1^*)s\}}{\lambda_1^* \lambda_2 (\lambda_2 - \lambda_1^*)}
\end{aligned}
\tag{5.6}
$$

$$
+ i \frac{|C_1|^2 |C_2|^2 \{|\lambda_1|^2 (\lambda_2 - \lambda_2^*) + |\lambda_2|^2 (\lambda_1 - \lambda_1^*)\} |\lambda_1 - \lambda_2|^4 \exp\{2i(\lambda_1 - \lambda_1^* + \lambda_2 - \lambda_2^*)s\}}{|\lambda_1|^2 |\lambda_2|^2 \{(\lambda_1 - \lambda_1^*)(\lambda_1 - \lambda_2^*)(\lambda_2 - \lambda_1^*)(\lambda_2 - \lambda_2^*)\}^2} ,
$$

with

$$
\begin{aligned}
C_1 &= C_1(0) \exp(4i\lambda_1^2 t) , \\
C_2 &= C_2(0) \exp(4i\lambda_2^2 t) .
\end{aligned}
\tag{5.7}
$$

We can consider a great variety of collision processes of a combination of lump, cusp and loop solitons with similar or dissimilar amplitudes traveling in the same direction or in the opposite direction. Profiles of these processes show very complex behavior as a consequence of the factor ε_+ and the period τ. Especially, complexity appears in collision of loop solitons. We show typical three cases:

(I) Collision of a large lump soliton and a small loop soliton,

(II) Head-on collision of two similar loop solitons,

(III) Bound state of two loop solitons.

Numerical results for the case (I) are illustrated in Figure 2 in which we can observe a small loop soliton with a positive velocity travels along a lump soliton with a negative velocity during the collision.

Figure 2

The profiles of collision process for the case (II) of the same loop solitons with the opposite velocities are illustrated in Figure 3 in which we can observe more complex movements of solitons just at the collision. After the collision two solitons separate in each other.

Figure 3

The case (III) is appeared if two solitons has the same velocities. We find the internal motion of the bound state as shown in Figure 4 where we take two similar loop solitons. We observe that one of the loop soliton periodically moves around another loop soliton. Here the real part of the two eigenvalues has the same value in the present case and its behaviour differs from the breather soliton known to the modified Korteweg-de Vries equation and the sine-Gordon equation.

Figure 4

§ 6 Discussions

In order to study the motion of soliton on the thin vortex filament, we have considered the modified WKI equation and obtained N soliton solution by means of the inverse scattering method. We introduced the sign function, which enabled us to get multivalued loop soliton solution, and transformed the independent variable from x to $s = x + \varepsilon_+$, which played a crucial role to obtain N soliton solution. We found, depending on the the ratio of the real and the imaginary parts of the eigenvalue, three kinds of vortex solutions such as lump, cusp and loop solitons.

We studied properties of one and two soliton solutions and analyzed intensively the typical collision processes. It would be worth to mention that our one vortex soliton is indeed observed in nature such as tornados*) and experiment of a rotating tank.[15] By comparing Figures 2, 3 and 4 with Figures 3, 4 and 6 of Reference 11, the readers will be convinced that our analysis on collision process of the vortex soliton in terms of Eq.(2.1) provides the theoretical foundation for the numerical observation of Aref and Flinchem for Eq.(2.9). Though Aref and Flinchem identified their numerical solutions as just transcriptions of solitons to the cubic nonlinear Schrödinger equation, one should notice, however, that the cubic nonlinear Schrödinger equation does not valid to describe large distortion of waves such as spiky solitons or multivalued loop solitons. Our soliton theory on the vortex motion will provide firm theoretical bases to investigate dynamic of the vortex filament under the action of external perturbations such as shear flow or viscosity.

*) The two photographs, one of which is very similar to Figure 1, are found in Reference 11.

References

1) For instance, see **Nonlinear Evolution Equations: Integrability and Spectral Method**, edited by A. Degasperis, A. Fordy and M. Lakshmanan (Manchester University Press) (1990) and **Nonlinear Evolution Equations and Dynamical Systems**, edited by S.Carillo and O.Ragnisco (Springer Verlag) (1990).
2) M.Wadati, K.Konno and Y.H.Ichikawa, **A generalization of the inverse scattering method**, J. Phys. Soc. Japan **46** 1965-1966 (1979).
3) M.Wadati, K.Konno and Y.H.Ichikawa, **New integrable evolution equations**, J. Phys. Soc. Japan **47** 1698-1700 (1979).
4) Y.H.Ichikawa, K.Konno and M.Wadati, **New Integrable Nonlinear Equations Leading to Exotic Solitons**, in **Long-Time Prediction in Dynamics**, edited by C.W.Horton, Jr., L.E.Reichl and V.G.Szebehely, (John Wiley & Sons) 345-365 (1983).
5) K.Konno and A. Jeffrey, **Some remarkable properties of two loop soliton solutions**, J. Phys. Soc. Japan **52** 1-3 (1983).
6) K.Konno and A. Jeffrey, **The Loop Soliton**, in **Advances in Nonlinear Waves Vol. I**, edited by L. Debnath, (Pitman Advanced Publishing Program) 162-183 (1984).
7) T. Shimizu and M. Wadati, **A new integrable nonlinear evolution equation**, Prog. Theor. Phys. **63** 808-820 (1980).
8) R.H. Hama, **Progressive deformation of a curved vortex filament by its own induction**, Phys. Fluids **5** 1156-1162 (1962).
9) H. Hashimoto, **A soliton on a vortex filament**, J. Fluid Mech. **51** 477-485 (1972).
10) D. Levi, A. Sym and S. Wojciechowski, **N-solitons on a vortex filament**, Phys. Letts. **94A** 408-411 (1983).
11) H. Aref and E.P. Flinchem, **Dynamics of a vortex filament in a shear flow**, J. fluid Mech. **148** 477-497 (1984).
12) K. Konno, **Relationship among modified WKI equation, equation of motion of a thin vortex filament and that of a continuous Heisenberg spin system**, J. Phys. Soc. Japan **59** (1990) No.10.
13) K. Konno, H.Sanuki and Y.H.Ichikawa, **Conservation laws of nonlinear-evolution equations**, Prog. Theor. Phys. **52** 886-889 (1974).
14) K. Konno, Y.H. Ichikawa and M. Wadati, **A loop soliton propagating along a stretched rope**, J. Phys. Soc. Japan **50** 1025-1026 (1981).
15) E.J. Hopfinger, F.K. Browand and Y. Gagne, **Turbulence and waves in a rotating tank**, J. Fluid Mech. **125** 505-534 (1982).

Figure Captions

Fig.1 Stereo view of one loop soliton solution and the shape of ε_+ for $\lambda = 0.5+i$ and $C(0) = 0.4038$, where the vertical line represents the x axis with the range of $-2 \leq x \leq 2$, the horizontal line the real q with the range of $-1 \leq \mathrm{Re}\, q \leq 1$ and $-1.5 \leq \varepsilon_+ \leq 0$. The imaginary axis is lined from the back of the paper to the front with the same range as the real q as $-1 \leq -\mathrm{Im}\, q \leq 1$. (A) $t = -0.3$, (B) 0 and (C) 0.3.

Fig.2 Stereo view of collision of one large lump and one small loop solitons for $\lambda_1 = 1 + 0.8i$, $C_1(0) = 1$, $\lambda_2 = -1 + 5i$ and $C_2(0) = 1$ where $-2 \leq x \leq 2$, $-0.5 \leq \mathrm{Re}\, q \leq 0.5$ and $-0.5 \leq -\mathrm{Im}\, q \leq 0.5$. (A) $t = -0.1$, (B) 0 and (C) 0.1.

Fig.3 Stereo view of collision of two loop solitons for $\lambda_1 = 0.5 + i$, $C_1(0) = i$, $\lambda_2 = -0.5 + i$ and $C_2(0) = i$ where $-2 \leq x \leq 2$, $-1 \leq \mathrm{Re}\, q \leq 1$ and $-1 \leq -\mathrm{Im}\, q \leq 1$. (A) $t = -0.3$, (B) 0 and (C) 0.3.

Fig.4 Stereo view of bound state of two loop solitons for $\lambda_1 = -0.5+2i$, $C_1(0) = 1$, $\lambda_2 = -0.5 + 3i$ and $C_2(0) = 1$ where $-2 \leq x \leq 2$, $-0.5 \leq \mathrm{Re}\, q \leq 0.5$ and $-0.5 \leq \mathrm{Im}\, q \leq 0.5$. (A) $t = -0.5$, (B) 0.15 and (C) 0.8.

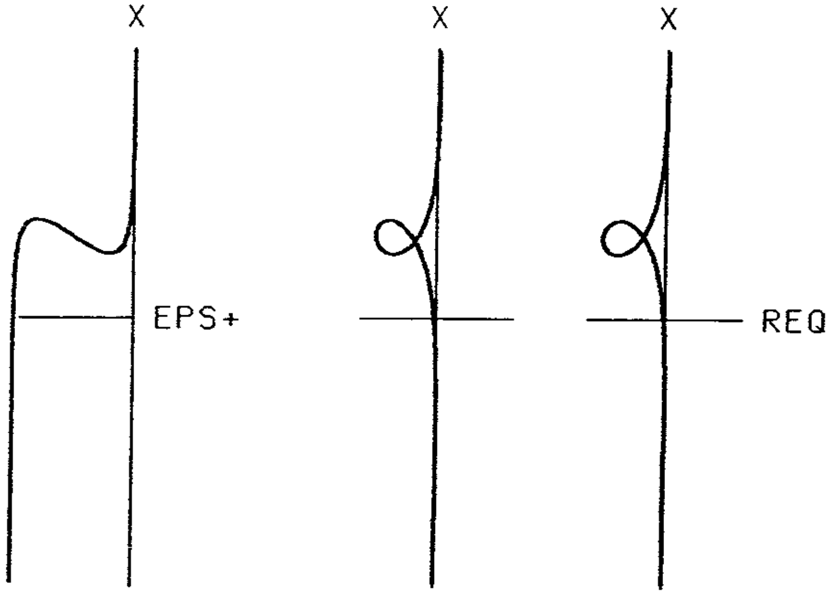

FIG.1
(A)

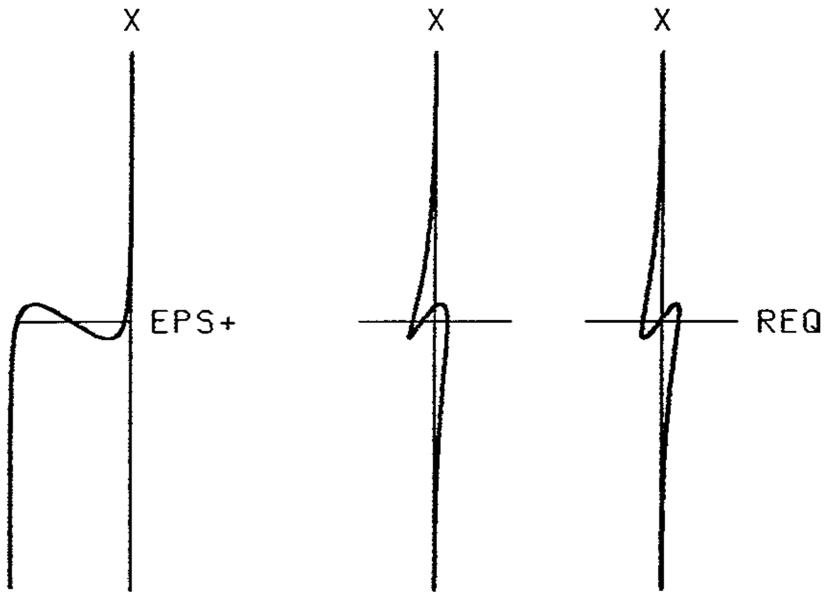

FIG.1
(B)

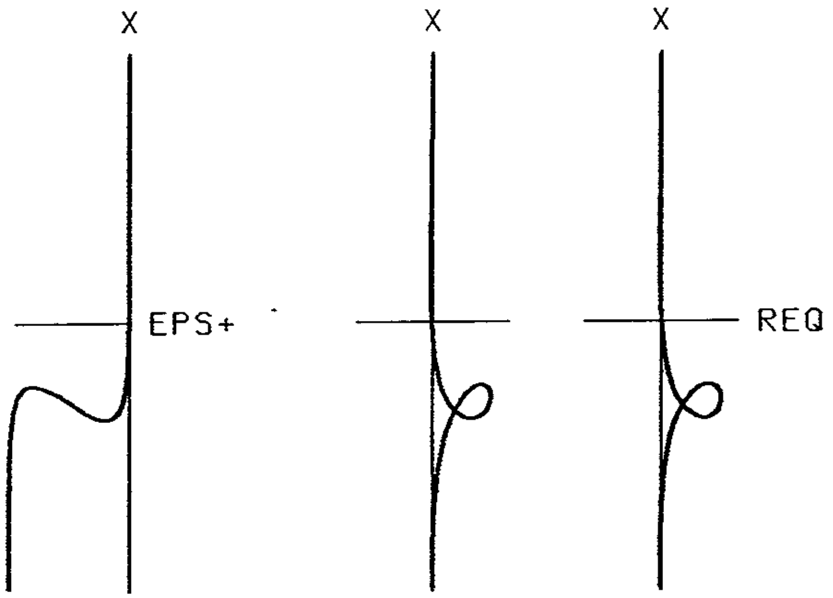

FIG.1
(C)

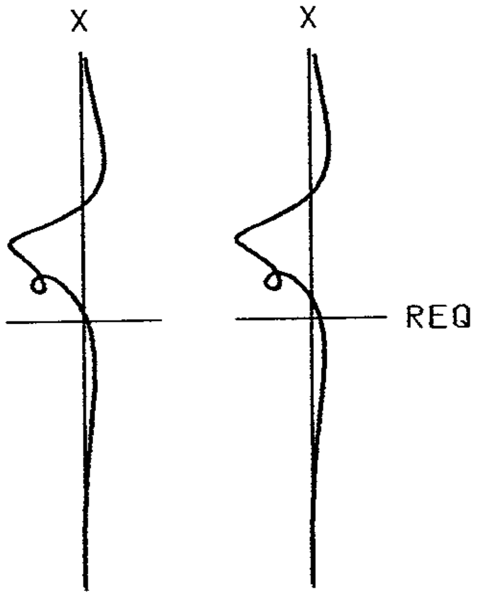

FIG.2
(A)

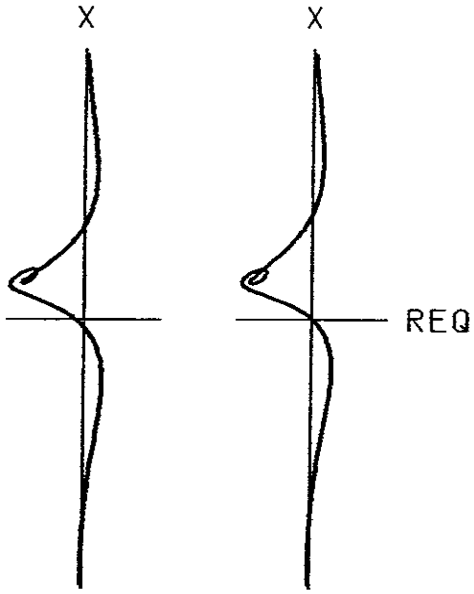

FIG.2
(B)

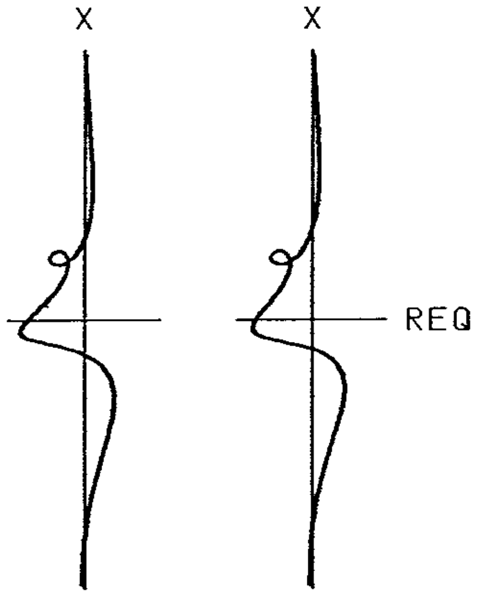

FIG.2
(C)

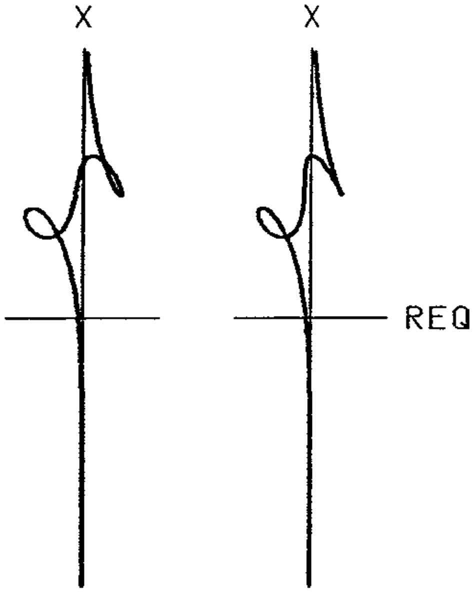

FIG.3
(A)

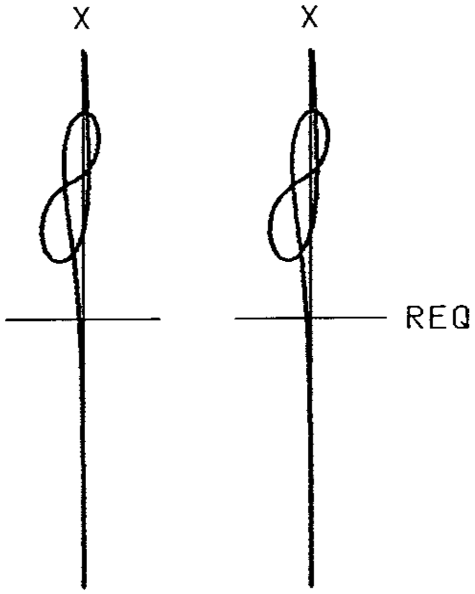

FIG.3
(B)

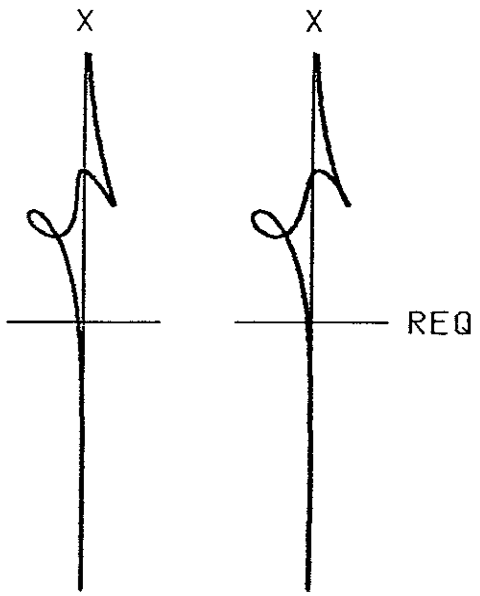

FIG.3
(C)

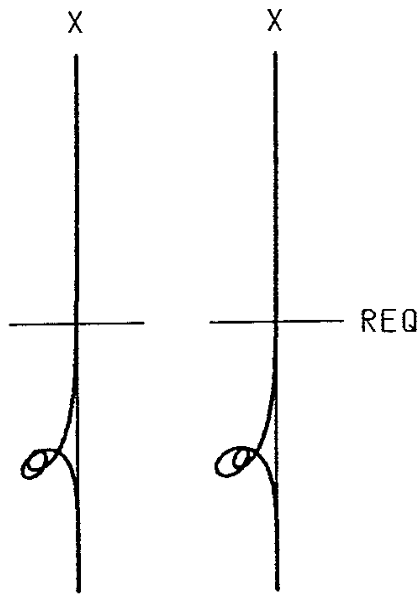

FIG.4
(A)

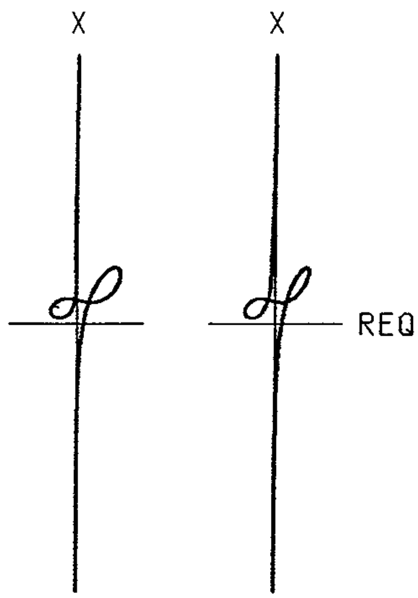

FIG.4
(B)

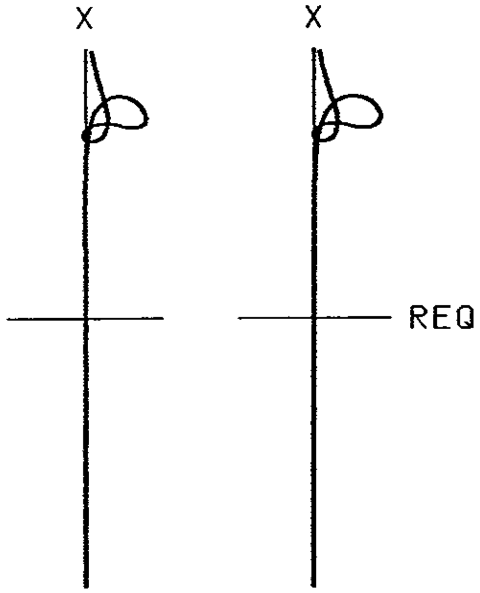

FIG.4
(C)

Recent Issues of NIFS Series

NIFS-30 K. Yamazaki, O. Motojima, M. Asao, M. Fujiwara and A. Iiyoshi, *Design Scalings and Optimizations for Super-Conducting Large Helical Devices* ; May 1990

NIFS-31 H. Sanuki, T. Kamimura, K. Hanatani, K. Itoh and J. Todoroki, *Effects of Electric Field on Particle Drift Orbits in a $l=2$ Torsatron* ; May 1990

NIFS-32 Yoshi H. Ichikawa, *Experiments and Applications of Soliton Physics*; June 1990

NIFS-33 S.-I. Itoh, *Anomalous Viscosity due to Drift Wave Turbulence* ; June 1990

NIFS-34 K. Hamamatsu, A. Fukuyama, S.-I. Itoh, K. Itoh and M. Azumi, *RF Helicity Injection and Current Drive* ; July 1990

NIFS-35 M. Sasao, H. Yamaoka, M. Wada and J. Fujita, *Direct Extraction of a Na- Beam from a Sodium Plasma* ; July 1990

NIFS-36 N. Ueda, S.-I. Itoh, M. Tanaka and K. Itoh, *A Design Method of Divertor in Tokamak Reactors* Aug. 1990

NIFS-37 J. Todoroki, *Theory of Longitudinal Adiabatic Invariant in the Helical Torus*; Aug. 1990

NIFS-38 S.-I. Itoh and K. Itoh, *Modelling of Improved Confinements – Peaked Profile Modes and H-Mode–* ; Sep. 1990

NIFS-39 O. Kaneko, S. Kubo, K. Nishimura, T. Syoji, M. Hosokawa, K. Ida, H. Idei, H. Iguchi, K. Matsuoka, S. Morita, N. Noda, S. Okamura, T. Ozaki, A. Sagara, H. Sanuki, C. Takahashi, Y. Takeiri, Y. Takita, K. Tsuzuki, H. Yamada, T. Amano, A. Ando, M. Fujiwara, K. Hanatani, A. Karita, T. Kohmoto, A. Komori, K. Masai, T. Morisaki, O. Motojima, N. Nakajima, Y. Oka, M. Okamoto, S. Sobhanian and J. Todoroki, *Confinement Characteristics of High Power Heated Plasma in CHS*; Sep. 1990

NIFS-40 K. Toi, Y. Hamada, K. Kawahata, T. Watari, A. Ando, K. Ida, S. Morita, R. Kumazawa, Y. Oka, K. Masai, M. Sakamoto, K. Adati, R. Akiyama, S. Hidekuma, S. Hirokura, O. Kaneko, A. Karita, T. Kawamoto, Y. Kawasumi, M. Kojima, T. Kuroda, K. Narihara, Y. Ogawa, K. Ohkubo, S. Okajima, T. Ozaki, M. Sasao, K. Sato, K.N. Sato, T. Seki, F. Shimpo, H. Takahashi, S. Tanahashi, Y. Taniguchi and T. Tsuzuki, *Study of Limiter H- and IOC- Modes by Control of Edge Magnetic Shear and Gas Puffing in the JIPP T-IIU Tokamak*; Sep. 1990

NIFS-41 K. Ida, K. Itoh, S.-I. Itoh, S. Hidekuma and JIPP T-IIU & CHS Group, *Comparison of Toroidal/Poloidal Rotation in CHS Heliotron/Torsatron and JIPP T-IIU Tokamak*; Sep .1990

NIFS-42 T.Watari, R.Kumazawa,T.Seki, A.Ando,Y.Oka, O.Kaneko, K.Adati, R.Ando, T.Aoki, R.Akiyama, Y.Hamada, S.Hidekuma, S.Hirokura, E.Kako, A.Karita, K.Kawahata, T.Kawamoto, Y.Kawasumi, S.Kitagawa, Y.Kitoh, M.Kojima, T. Kuroda, K.Masai, S.Morita, K.Narihara, Y.Ogawa, K.Ohkubo, S.Okajima, T.Ozaki, M.Sakamoto, M.Sasao, K.Sato, K.N.Sato, F.Shinbo, H.Takahashi, S.Tanahashi, Y.Taniguchi, K.Toi, T.Tsuzuki, Y.Takase, K.Yoshioka, S.Kinoshita, M.Abe, H.Fukumoto, K.Takeuchi, T.Okazaki and M.Ohtuka, ,*Application of Intermediate Frequency Range Fast Wave to JIPP T-IIU and HT-2 Plasma*; Sep. 1990

NIFS-43 K.Yamazaki, N.Ohyabu, M.Okamoto, T.Amano, J.Todoroki, Y.Ogawa, N.Nakajima, H.Akao, M.Asao, J.Fujita, Y.Hamada, T.Hayashi, T.Kamimura, H.Kaneko, T.Kuroda, S.Morimoto, N.Noda, T.Obiki, H.Sanuki, T.Sato, T.Satow, M.Wakatani, T.Watanabe, J.Yamamoto, O.Motojima, M.Fujiwara, A.Iiyoshi and LHD Design Group, *Physics Studies on Helical Confinement Configurations with l=2 Continuous Coil Systems*; Sep. 1990

NIFS-44 T.Hayashi, A.Takei, N.Ohyabu, T.Sato, M.Wakatani, H.Sugama, M.Yagi, K.Watanabe, B.G.Hong and W.Horton, *Equilibrium Beta Limit and Anomalous Transport Studies of Helical Systems*; Sep. 1990

NIFS-45 R.Horiuchi, T.Sato, and M.Tanaka, *Three-Dimensional Particle Simulation Study on Stabilization of the FRC Tilting Instability*; Sep. 1990

NIFS-46 K.Kusano, T.Tamano and T. Sato, *Simulation Study of Nonlinear Dynamics in Reversed-Field Pinch Configuration*; Sep. 1990

NIFS-47 Yoshi H.Ichikawa, *Solitons and Chaos in Plasma*; Sep. 1990

NIFS-48 T.Seki, R.Kumazawa, Y.Takase, A.Fukuyama, T.Watari, A.Ando, Y.Oka, O.Kaneko, K.Adati, R.Akiyama, R.Ando, T.Aoki, Y.Hamada, S.Hidekuma, S.Hirokura, K.Ida, K.Itoh, S.-I.Itoh, E.Kako, A. Karita, K.Kawahata, T.Kawamoto, Y.Kawasumi, S.Kitagawa, Y.Kitoh, M.Kojima, T.Kuroda, K.Masai, S.Morita, K.Narihara, Y.Ogawa, K.Ohkubo, S.Okajima, T.Ozaki, M.Sakamoto, M.Sasao, K.Sato, K.N.Sato, F.Shinbo, H.Takahashi, S.Tanahashi, Y.Taniguchi, K.Toi and T.Tsuzuki, *Application of Intermediate Frequency Range Fast Wave to JIPP T-IIU Plasma*; Sep.1990

NIFS-49 A.Kageyama, K.Watanabe and T.Sato, *Global Simulation of the Magnetosphere with a Long Tail: The Formation and Ejection of Plasmoids*; Sep.1990

NIFS-50 S.Koide, *3-Dimensional Simulation of Dynamo Effect of Reversed Field Pinch*; Sep. 1990

NIFS-51 O.Motojima, K. Akaishi, M.Asao, K.Fujii, J.Fujita, T.Hino, Y.Hamada, H.Kaneko, S.Kitagawa, Y.Kubota, T.Kuroda, T.Mito, S.Morimoto, N.Noda, Y.Ogawa, I.Ohtake, N.Ohyabu, A.Sagara, T. Satow, K.Takahata, M.Takeo, S.Tanahashi, T.Tsuzuki, S.Yamada, J.Yamamoto, K.Yamazaki, N.Yanagi, H.Yonezu, M.Fujiwara, A.Iiyoshi and LHD Design Group, *Engineering Design Study of Superconducting Large Helical Device*; Sep. 1990

NIFS-52 T.Sato, R.Horiuchi, K. Watanabe, T. Hayashi and K.Kusano, *Self-Organizing Magnetohydrodynamic Plasma*; Sep. 1990

NIFS-53 M.Okamoto and N.Nakajima, *Bootstrap Currents in Stellarators and Tokamaks*; Sep. 1990

NIFS-54 K.Itoh and S.-I.Itoh, *Peaked-Density Profile Mode and Improved Confinement in Helical Systems*; Oct. 1990

NIFS-55 Y.Ueda, T.Enomoto and H.B.Stewart, *Chaotic Transients and Fractal Structures Governing Coupled Swing Dynamics*; Oct. 1990

NIFS-56 H.B.Stewart and Y.Ueda, *Catastrophes with Indeterminate Outcome*; Oct. 1990

NIFS-57 S.-I.Itoh, H.Maeda and Y.Miura, *Improved Modes and the Evaluation of Confinement Improvement*; Oct. 1990

NIFS-58 H.Maeda and S.-I.Itoh, *The Significance of Medium- or Small-size Devices in Fusion Research*; Oct. 1990

NIFS-59 A.Fukuyama, S.-I.Itoh, K.Itoh, K.Hamamatsu, V.S.Chan, S.C.Chiu, R.L.Miller and T.Ohkawa, *Nonresonant Current Drive by RF Helicity Injection*; Oct. 1990

NIFS-60 K.Ida, H.Yamada, H.Iguchi, S.Hidekuma, H.Sanuki, K.Yamazaki and CHS Group, *Electric Field Profile of CHS Heliotron/Torsatron Plasma with Tangential Neutral Beam Injection*; Oct. 1990

NIFS-61 T.Yabe and H.Hoshino, *Two- and Three-Dimensional Behavior of Rayleigh-Taylor and Kelvin-Helmholz Instabilities*; Oct. 1990

NIFS-62 H.B. Stewart, *Application of Fixed Point Theory to Chaotic Attractors of Forced Oscillators;* Nov. 1990

NIFS DATA-1 Y. Yamamura, T. Takiguchi and H. Tawara, *Data Compilation of Angular Distributions of Sputtered Atoms* ; Jan. 1990

NIFS DATA-2 T. Kato, J. Lang and K. E. Berrington, *Intensity Ratios of Emission Lines from OV Ions for Temperature and Density Diagnostics* ; Mar. 1990

NIFS DATA-3 T. Kaneko, *Partial Electronic Straggling Cross Sections of Atoms for Protons* ; Mar. 1990

NIFS DATA-4 T. Fujimoto, K. Sawada and K. Takahata, *Cross Section for Production of Excited Hydrogen Atoms Following Dissociative Excitation of Molecular Hydrogen by Electron Impact* ; Mar. 1990

NIFS DATA-5 H. Tawara, *Some Electron Detachment Data for H- Ions in Collisions with Electrons, Ions, Atoms and Molecules – an Alternative Approach to High Energy Neutral Beam Production for Plasma Heating–* ; Apr. 1990

NIFS DATA-6 H. Tawara, Y. Itikawa, H. Nishimura, H. Tanaka and Y. Nakamura, *Collision Data Involving Hydro-Carbon Molecules* ; July 1990

NIFS DATA-7 H.Tawara, *Bibliography on Electron Transfer Processes in Ion-Ion/Atom/Molecule Collisions –Updated 1990–*; Oct. 1990

NIFS TECH-1 H. Bolt and A. Miyahara, *Runaway–Electron –Materials Interaction Studies* ; Mar. 1990

NIFS PROC-1 *U.S.-Japan Workshop on Comparison of Theoretical and Experimental Transport in Toroidal Systems Oct. 23-27, 1989* ; Mar. 1990

NIFS PROC-2 *Structures in Confined Plasmas –Proceedings of Workshop of US-Japan Joint Institute for Fusion Theory Program–* ; Mar. 1990

NIFS PROC-3 *Proceedings of the First International Toki Conference on Plasma Physics and Controlled Nuclear Fusion –Next Generation Experiments in Helical Systems– Dec. 4-7, 1989* ; Mar. 1990

NIFS PROC-4 *Plasma Spectroscopy and Atomic Processes –Proceedings of the Workshop at Data & Planning Center in NIFS–*; Sep. 1990

NIFS PROC-5 *Symposium on Development of Intensed Pulsed Particle Beams and Its Applications*; Oct. 1990